arXiv:1609.02352v1 [cond-mat.quant-gas] 8 Sep 2016

Quantum Magnetism with Mesoscopic Bose-Einstein Condensates

A. Gallemí,[1,2] G. Queraltó,[3] M. Guilleumas,[1,2] R. Mayol,[1,2] and A. Sanpera[3,4]

[1]*Departament de Física Quàntica i Astrofísica, Universitat de Barcelona, E–08028 Barcelona, Spain*
[2]*Institut de Nanociència i Nanotecnologia de la Universitat de Barcelona, IN^{2}UB, E–08028 Barcelona, Spain*
[3]*Departament de Física, Universitat Autònoma de Barcelona, E–08193 Bellaterra, Spain*
[4]*Institució Catalana de Recerca i Estudis Avançats, ICREA, E–08011 Barcelona, Spain*

(Dated: September 9, 2016)

Lattice gases in the strongly correlated regime have been proven to simulate quantum magnetic models under certain conditions: the mapping of the double-well system onto the Lipkin-Meshkov-Glick spin model is a paradigmatic case. A suitable definition of the length in the Hilbert space of the system leads to the concept of a correlation length, whose divergence is a characteristic property of continuous quantum phase transitions. We calculate the finite-size scaling of some observables like e.g. the magnetization or the population imbalance, as well as of the Schmidt gap, obtaining in this way the critical exponents associated to such transitions. The systematic definition of the Schmidt gap in extended Hamiltonians provides a good tool to analyze the set of critical exponents associated to transitions in systems formed by a larger number of traps. This demonstrates, thus, the potential use of mesoscopic Bose-Einstein condensates as quantum simulators of condensed matter systems.

PACS numbers: 03.75.Hh, 03.75.Lm, 03.75.Gg, 67.85.-d

I. INTRODUCTION

The achievement of quantum magnetism with ultracold lattice atoms can be regarded as one of the cornerstones of modern physics. Indeed, the seminal proposal [1] that ultracold atoms confined in optical lattices can be described by a Bose-Hubbard model [2], together with the experimental signatures of the superfluid-Mott insulator quantum phase transition in such systems [3] have prompted the field of quantum simulators. Since then, the scope of condensed matter phenomena that can be addressed with ultracold gases and ions has broadened enormously (see e.g [4–7] and references therein).

One of the paradigmatic models of strongly correlated states in condensed matter are the family of Hubbard Hamiltonians. These Hamiltonians describe, in a very simplified way, magnetic properties of some materials. Ultracold atoms loaded in optical lattices can realize, almost perfectly, many of such Hamiltonians. For instance, the Mott insulator phase of the Bose-Hubbard model is achieved by "freezing" at each lattice site a single atom. In certain limits, the Hubbard Hamiltonians reduce to various spin models: an exemplary case is the non-interacting XY spin model, which has been simulated with hard-core bosons in optical lattices [8]. A generic constraint to realize interacting spin models with ultracold lattice atoms is the extreme low temperature required, going down to the picoKelvin regime. The reason is that these spin models are derived as second order perturbation theory from Hubbard models, and temperature scales then as t^2/U [9], where t denotes tunneling between nearest sites and U is the atomic two-body on-site interaction.

Here, we take a different path to show that quantum magnetism can also be approached using mesoscopic (dipolar) Bose-Einstein condensates constituted by few cents of atoms confined in few (for the sake of simplicity we restrict to two and three) harmonic traps. In these systems, the relevant temperature is the critical temperature for degeneracy, which in the double-well potential is of the order of tens or hundreds of nanoKelvins, relaxing substantially the temperature constraints required by atoms in optical lattices to simulate spin models. Our main result is to show that these systems can be used to simulate quantum magnetism and, in particular, quantum phase transitions.

Our manuscript is organized as follows. In Section II we review first the mean-field description of a condensate in a double-well potential, and the regime for which the mean-field description fails due to the presence of a quantum phase transition. In Section III we analyze the quantum phase transition from a quantum magnetism perspective linking our results to key concepts like correlation length, critical exponents and universality, which are well defined in spin models, like the Ising model. We complement our study by analyzing these quantum phase transitions from an entanglement perspective. In Section IV, we extend our studies to dipolar condensates confined in three wells and show the meaning of universality classes in such systems. In Section V we present our conclusions and open questions.

II. MESOSCOPIC CONDENSATES IN A DOUBLE-WELL POTENTIAL

The description of mesoscopic ultracold Bose-Einstein condensates confined in few-well potentials has been addressed in great detail both experimentally [10–12] and theoretically, see e.g. [13] and references therein. In the weakly interacting regime, these mesoscopic systems can be described within a Hartree approach in which all particles share a common state (the condensate wavefunction) and the dynamics at low temperatures can then be

accurately reproduced with the time-dependent Gross-Pitaevskii equation. For a double-well potential, the description of the system can be further simplified with the so-called two-mode approximation, where the population imbalance and the phase difference between the condensates on each well are enough to capture the physics displayed by the system. Such mean field description, nevertheless, fails drastically when the interaction strength between atoms approaches some critical value. At this moment, the Gross-Pitaevskii solution breaks the symmetry of the double-well potential and becomes highly unstable [14]. In these cases, the Bogoliubov approach shows a divergence in the number of atoms in the non-condensate modes [15]. In such regime, an accurate description of the system is a simplified Bose-Hubbard Hamiltonian where each trap corresponds now to a mode or site.

In what follows we consider N spinless bosons trapped in M sites, which we restrict to be $M \leq 3$, although our study could be generalized to higher M. We further assume that atoms might have an electric or magnetic dipole moment $\boldsymbol{d}$, all of them polarized along the same direction by the presence of an external strong field. Bosons interact via short range potentials but also, when present, with dipolar long-range interactions that couple bosons in different traps. The bosonic field operators that annihilate (create) a boson at a point $\boldsymbol{r}$ are defined as $\hat{\psi}(\boldsymbol{r}) = \sum_i \phi_i(\boldsymbol{r})\, \hat{a}_i$, where as usual $\hat{a}_i(\,\hat{a}_i^\dagger)$ is the bosonic annihilation (creation) operator on trap i fulfilling canonical commutation relations $[\hat{a}_i^\dagger, \hat{a}_j] = \delta_{ij}$. Under these assumptions, the extended Bose-Hubbard Hamiltonian reads:

$$\hat{H} = -\frac{t}{2}\sum_i \left[\hat{a}_i^\dagger \hat{a}_{i+1} + h.c.\right] + \frac{U}{2}\sum_i \hat{n}_i(\hat{n}_i - 1) + \sum_{i\neq j} U_{ij}\, \hat{n}_i \hat{n}_j\,, \tag{1}$$

where $\hat{n}_i = \hat{a}_i^\dagger \hat{a}_i$ is the particle number operator on i-th well, and $\sum_i \hat{n}_i = N$. In Eq. (1), the indices i, j run for all the lattice sites. The Hamiltonian (1) is characterized by three parameters: the tunneling rate t between adjacent wells, the onsite energy U, which includes both contact and dipole-dipole interactions, and the intersite energy U_{ij}, which takes into account the long range and anisotropy of the dipolar interaction. We notice here that for a double-well potential the effects of dipolar interactions can be included into a rescaled contact interaction, and the Hamiltonian reduces to the non-dipolar case [16]. The structure of the above Hamiltonian makes it convenient to work in the Fock basis $|F\rangle_{n_1,n_2,...,n_M} = |n_1, n_2, ..., n_M\rangle = |n_1\rangle \otimes |n_2\rangle \otimes \cdots \otimes |n_M\rangle$ that labels the number of atoms in each well. Then, the wavefunction can be written as $|\Psi\rangle = \sum_{n_i} C_{n_1,n_2,...,n_M}\, |F\rangle_{n_1,n_2,...,n_M}$. The ground state solution is obtained by exact diagonalization of Eq. (1), for different values of N, t and U.

For simplicity we consider first the double-well potential. In this case, the Schwinger representation allows to map the two-mode annihilation and creation operators onto spin operators:

$$\begin{aligned} \hat{S}_+ &= \hat{a}_1^\dagger \hat{a}_2, \\ \hat{S}_- &= \hat{a}_2^\dagger \hat{a}_1, \\ \hat{S}_z &= \frac{1}{2}(\hat{a}_1^\dagger \hat{a}_1 - \hat{a}_2^\dagger \hat{a}_2), \end{aligned} \tag{2}$$

with the constraint $\hat{a}_1^\dagger \hat{a}_1 + \hat{a}_2^\dagger \hat{a}_2 = 2\hat{S} = \hat{N}$, which fixes the total number of bosons or equivalently the total spin. Using such representation, the two-site Bose-Hubbard Hamiltonian can be rewritten as

$$\begin{aligned} \hat{H}_{DW} &= -\frac{t}{2}(\hat{S}_+ + \hat{S}_-) + U(\hat{S}_z^2 + \hat{S}^2 - \hat{S}) \\ &= -t\hat{S}_x + U\,\hat{S}_z^2, \end{aligned} \tag{3}$$

where in the last equation, we have used that $[\hat{H}_{DW}, \hat{N}] = [\hat{H}_{DW}, \hat{S}] = 0$ to remove all terms proportional to the total spin $\hat{S}$. By defining $\hat{S}_\alpha = \sum_{i=1}^N \hat{\sigma}_i^\alpha/2$ as the collective spin along the α-direction, where the set of operators σ^α corresponds to the Pauli matrices, the double-well Hamiltonian $\hat{H}_{DW}$ can be interpreted as a system of N spin-1/2 particles mutually interacting along the z-axis and embedded in a transverse magnetic field along the x-direction. Thus, the double-well Hamiltonian (3) is just a particular case of the general Lipkin-Meshkov-Glick model [17] introduced long time ago in nuclear physics to study quantum phase transitions (QPTs) in "mean field" models, where all spins interact to each other, and since then exploited in many different contexts e.g. [18–21]. The corresponding Hamiltonian is:

$$\hat{H}_{LMG} = -h\sum_i \hat{\sigma}_i^x - \frac{\lambda}{N}\sum_{i<j}\left(\hat{\sigma}_i^z\hat{\sigma}_j^z + \gamma\hat{\sigma}_i^y\hat{\sigma}_j^y\right), \tag{4}$$

where the factor $1/N$ ensures the convergence of the free energy per spin in the thermodynamic limit (TL) $N \to \infty$. This magnetic model and its corresponding phase transitions have been very well studied. For $\lambda > 0$, i.e. when the interaction between spins is ferromagnetic, there exists a second order phase transition at $\lambda = |h|$, if $0 \leq \gamma \leq 1$. Thus, approaching $|U|N/t \to 1$, there is a QPT between ferromagnetic and paramagnetic order, which in the TL converges to $|U|/t \to 0$. The paramagnetic region is thus proportional to $1/N$, non-degenerate and has a gap that vanishes at criticality. We notice that in the double-well potential, the TL corresponds to the limit in which a mean field description is valid and does not require to reach $N \to \infty$ but rather a sufficiently large N. Finally, we remark that in these models, in which each particle interacts with each other, the dimension of the Hilbert space is infinite (mean field) and the concept of length is not defined.

III. CORRELATION LENGTH AND CRITICAL EXPONENTS IN A DOUBLE-WELL POTENTIAL

As already mentioned, when approaching the limit $|U|N/t \to 1$, the mean field description of the double well collapses and the Gross-Pitaevskii equation cannot provide anymore the description of the ground state of the system. The two-well Bose-Hubbard description shows also a massive fluctuation of the particle number on each well in the border of the transition regime. Indeed, it is the existence of quantum fluctuations on all length scales, the most characteristic feature of (continuous) QPTs occurring at zero-temperature. This behavior, commonly denoted as criticality, is also reflected on the behavior of some observables $\hat{O}$ that scale near the transition point $|U_{crit}| = t/N$ as a power law $\hat{O} \propto |U - U_{crit}|^{\alpha}$, where α is a set of parameters called critical exponents that determine the qualitative nature of the critical behavior. Those parameters α are independent of the microscopic details of the system, but are rather linked to the symmetries of the emerging order as well as to the dimensionality of the system. Thus, QPTs associated to different Hamiltonians that share the same set of critical exponents are said to belong to the same universality class. The QPT is also accompanied by the vanishing of some energy scale and the divergence of some length (the correlation length) which indicates the spread of correlations in the system [22].

We aim at interpreting the QPTs in the double-well potential in a similar way as in spin chains, provided a definition of correlations. This definition allows to link critical behavior to the divergence of a correlation length. With this purpose we first calculate the phase diagram of the double well for different values of N near criticality. Inspired by two-point correlations in spin chains, we define correlations in our system in such a way that their behavior properly displays the relevant features of the QPTs. Then, we analyze the scaling behavior of some operators and perform finite-size scaling (see below) to obtain the corresponding critical exponents. Finally, we check if other models of the restricted Bose-Hubbard family share the same critical exponents and belong, therefore, to the same universality class.

Notice that in a spin chain of spin $\boldsymbol{S}$ particles, the length is naturally settled by the number of sites L (number of spins), and two-body spin-spin correlations are given by $\mathcal{C}_{ij} = \langle \boldsymbol{S}_i \boldsymbol{S}_j \rangle - \langle \boldsymbol{S}_i \rangle \langle \boldsymbol{S}_j \rangle$. Translational invariance in such systems ensures that the behavior of spin-spin correlations depends only on the distance between the two sites $|i-j|$, but not on the specific sites i, j. This fact allows to define a correlation length ξ, which fixes the length scale at which the spins are correlated between them. Far from criticality, the decay of correlations is exponential $\mathcal{C}_{ij} \sim \exp(-|i-j|/\xi)$, meaning that two far away spins are not correlated. At criticality, for continuous second order phase transitions, the decay is algebraic $\mathcal{C}_{ij} \sim (|i-j|^{-(d-2+\eta)})$, where d is the dimension, and the correlation length diverges as $\xi \propto |U - U_{crit}|^{-\nu}$, where

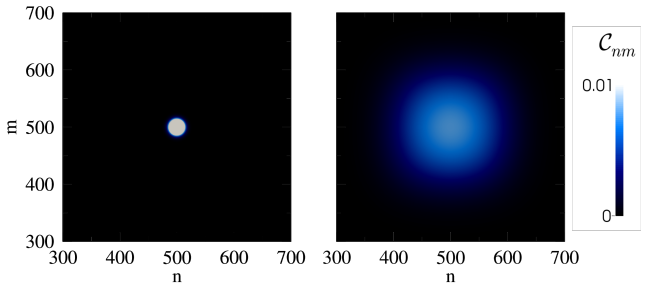

FIG. 1: Behavior of the correlations $\mathcal{C}_{nm}$ as a function of n and m for a double well. Left panel: $UN/t = 100$ far from criticality; right panel: $UN/t = -1$, at criticality. The figures correspond to $N = 1000$, thus, the ground state corresponds to 500 atoms in each well (in the center of color map).

U_{crit} is the critical point, expressing the fact that now spins are correlated between them even when they are far.

In a double well, such length scale is obviously irrelevant. In order to mimic the behavior of second order QPTs in spin chains in our system, we start by realizing that the quantity that settles the dimension of the Hilbert space here is the number of bosons on each well. Furthermore, this permits to order the Fock states in the following way: $|N,0\rangle, |N-1,1\rangle, \cdots, |0,N\rangle$. We then define two-body correlations in the ground state of our system as:

$$\begin{aligned} G_{nm} &= \sum_{|n-m|} \frac{\langle\, |n\rangle \langle m| \otimes |N-n\rangle \langle N-m|\,\rangle}{|n-m|} \\ &= \sum_{|n-m|} \frac{\mathcal{C}_{nm}}{|n-m|}\,, \end{aligned} \tag{5}$$

where the operator $|n\rangle \langle m|$ acts on the first trap and $|N-n\rangle \langle N-m|$ on the second one. So, we analyze how the number of bosons are correlated within a trap, i.e. the simultaneous presence of n and m bosons in the ground state and the sum extends over all possible contributions with $|n-m|$ fixed. Notice that $\mathcal{C}_{nm}$ is not equivalent to the widely used population imbalance operator in the double-well potential. The latter indicates the difference of population between the wells and corresponds to the expectation value of the population imbalance $Z = \langle \hat{S}_z \rangle = \langle |\hat{n}_1 - \hat{n}_2| \rangle / N = \sum_{n_1,n_2} |C_{n_1,n_2}|^2 (|n_1 - n_2|)/N$, while the former, $\mathcal{C}_{nm} = C_{n,N-n} C_{m,N-m}$, correlates boson occupation numbers within a well. In order to recover the "translational invariance", concept rooted in spin chains, we weight the correlation function by the "effective distance" $|n-m|$. This renormalization factor ensures the proper behavior of correlations as it neglects contributions from any intermediate level between n and m.

The general behavior of the correlations $\mathcal{C}_{nm}$ as a function of n and m, far from and close to criticality, is shown in Fig. 1, in the left and right panel, respectively. While far from criticality, the ground state is correlated with

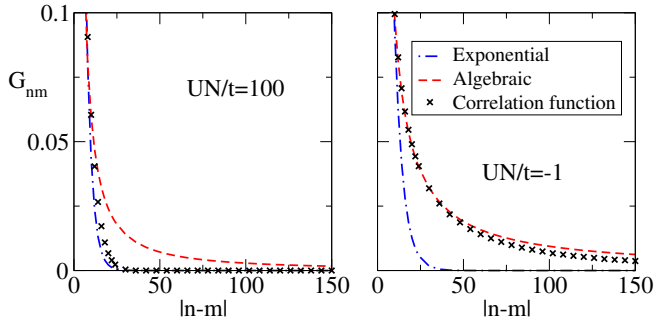

FIG. 2: Correlation function for the double-well potential G_{nm} versus $|n-m|$. Left panel: $UN/t = 100$ far from criticality. Right panel: $UN/t = -1$ at the critical point. The figures correspond to $N = 1000$. To better understand the different behavior far and close to criticality, an exponential decay (dashed-dotted line) and an algebraic decay (dashed line) has been drawn to guide the eye. As clearly displayed in the figure, at criticality (right panel) the best adjustment is algebraic, otherwise it is exponential (left panel).

the closer states only, at criticality the spreading of correlations becomes evident. Nevertheless, it is indeed the weighted function G_{nm} the one which allows to recover the concept of "translational invariance" and define a correlation length ξ for the system. In Fig. 2, we display G_{nm} as a function of $|n-m|$ far from and near criticality. One can see that G_{nm} decays exponentially far from the critical point and algebraically at criticality. To better stress the character of the correlation decay we fit the functions by an exponential and a power law.

To obtain a deeper understanding about the concept of correlation and the exact location of the QPT in the mean field limit, we analyze the behavior of the population imbalance Z, its fluctuations ΔZ, the magnetization along the z-axis, defined as $m_z = (\langle \hat{S}_z^2 \rangle)^{1/2}/N$ [19], and the entanglement spectrum. The latter is defined as the eigenvalues of the reduced density matrix of one mode or trap $\hat{\rho}_L = \mathrm{Tr}_R |\Psi\rangle\langle\Psi| = \sum \lambda_i |u_i\rangle\langle u_i|_L$ where $L(R)$ stands for the left (right) trap in the double-well configuration and λ_i are the eigenvalues of the Schmidt decomposition. The difference between the two largest non-degenerate Schmidt eigenvalues of the entanglement spectrum $\Delta\lambda = \lambda_1 - \lambda_2$, is called the Schmidt gap, and it closes at the critical point in the TL [23, 24].

In spin chains, finite-size effects strongly modify the location of the critical point where a quantum phase transition occurs, while distorts the general properties of the transition [25]. In order to do that, we repeat our simulations for different number of atoms $N = 500, 1000, 1500$ and look at the exponents that make all data to cross (critical point), and to collapse in order to obtain the critical exponents of observables, which scale as $\hat{O} \simeq N^{-\beta/\nu} f(|U - U_{crit}|N^{1/\nu})$, where ν is the mass gap exponent (associated to the correlation length divergence), and β is the critical exponent of the corresponding operator $\hat{O}$. In Fig. 3 we display the scaling behavior of

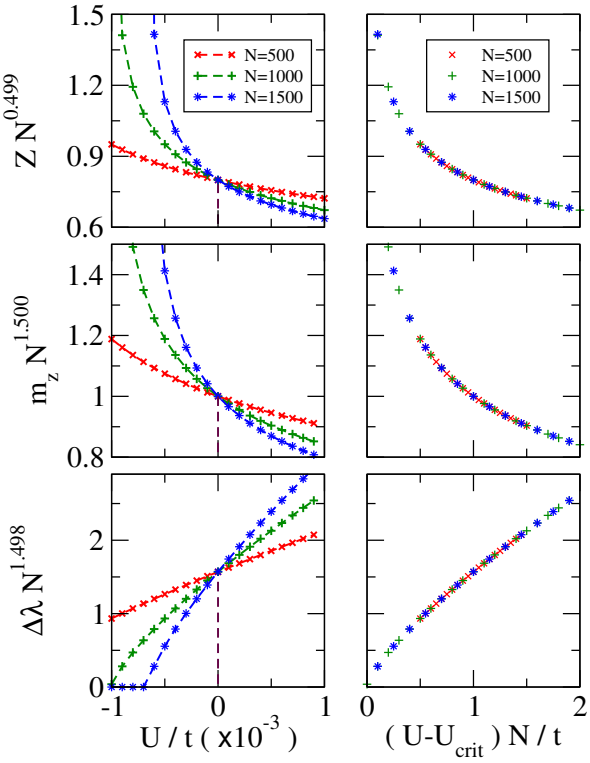

FIG. 3: Finite-size scaling behavior of the population imbalance (first row), the magnetization along the z-axis (second row) and the Schmidt gap (third row) in the double-well potential. The critical exponents obtained via this method are summarized in Table I.

the population imbalance Z, the magnetization along the z-axis, and the Schmidt gap for the double-well case. Despite the fact that $\Delta\lambda$ is not an observable, all quantities exhibit scaling, which allows us to extract the critical exponents, which are summarized in Table I.

	Z	ΔZ	m_z	$\Delta\lambda$
ν	1.000	1.000	1.000	1.000
β	0.499	0.502	1.500	1.498

TABLE I: Critical exponents of the correlation length (ν) and the scaling operator (β) obtained from the scaling of the population imbalance (Z), its fluctuations (ΔZ), the magnetization along the z-direction m_z, and the Schmidt gap $\Delta\lambda$ (obtained from the entanglement spectrum).

As expected, from the scaling of population imbalance, we obtain the mean-field exponents for S_z and the mass gap, which converge to $\beta = 1/2$ and $\nu = 1$ in agreement with previous works [20, 26]. Interestingly, the critical exponents obtained from the scaling of the magnetization m_z and the entanglement spectrum $\Delta\lambda$ coincide and result into $\beta = 3/2$ and $\nu = 1$ in agreement with [18, 19].

IV. QUANTUM PHASE TRANSITIONS IN THE EXTENDED BOSE-HUBBARD HAMILTONIAN: UNIVERSALITY

We have seen in the previous section that the second order QPT that appears in the phase diagram of the double-well system, can be accurately described in terms of a correlation function inspired by a spin model like the Ising spin chain. The reinterpretation of the occupation number on each well as an effective length in the corresponding Hilbert space allows to provide scaling properties of some important observables like population imbalance, magnetization along a given axis or the Schmidt gap. In turn, the scaling properties of such observables lead to the a set of critical exponents that can be associated to the corresponding quantum phase transition. A natural question arises when the number of wells is increased: Does the same analysis hold outside of the double-well configuration?

In this section, we focus on the study of the solutions of the extended Bose-Hubbard Hamiltonian given by (1) for the triple-well configuration, including now the role of dipolar interactions. Depending on the geometry of the wells, and the polarization orientation, the system will display the anisotropy and the long range of the dipolar interaction. Three cases, which are particularly appealing for our aim, have been studied. The first one corresponds to the three sites constituting a triangular geometry with no dipolar interaction [27] (see the inset of the top-right panel of Fig. 4), which owns a QPT at negatives values of the on-site interaction [28], analogous to the double-well case. The second one corresponds to the same triangular geometry holding dipolar atoms, with all the dipoles oriented along the direction defined by two of the sites, according to the inset of the middle-right panel of Fig. 4. Under this polarization orientation, the system exhibits a QPT, where one of the sites, is empty, and the system behaves effectively as a double well [29]. Finally, the third case concerns a three-well linear configuration with all sites aligned along the polarization direction of the dipoles [30], as shown in the inset of the bottom-right panel of Fig. 4. The phase diagram of this system presents a QPT at negatives values of the on-site interaction, and the system transits from a state where all the atoms are in the central well, to another state where half of the atoms are in the central site and the other half macroscopically occupies one of the external wells, constituting a cat state.

In the double-well case, we have analyzed the scaling properties of some observables, like the imbalance, its fluctuations and the magnetization. For the triple-well case, the definition of the equivalent observables is not so straightforward. Nevertheless, the Schmidt gap can be computed in the way commented before, and we can take profit from its scaling properties. In three-well systems, however, there are more than a single partition of the system (remember that the Schmidt decomposition only works for bipartite systems). In particular, the last two

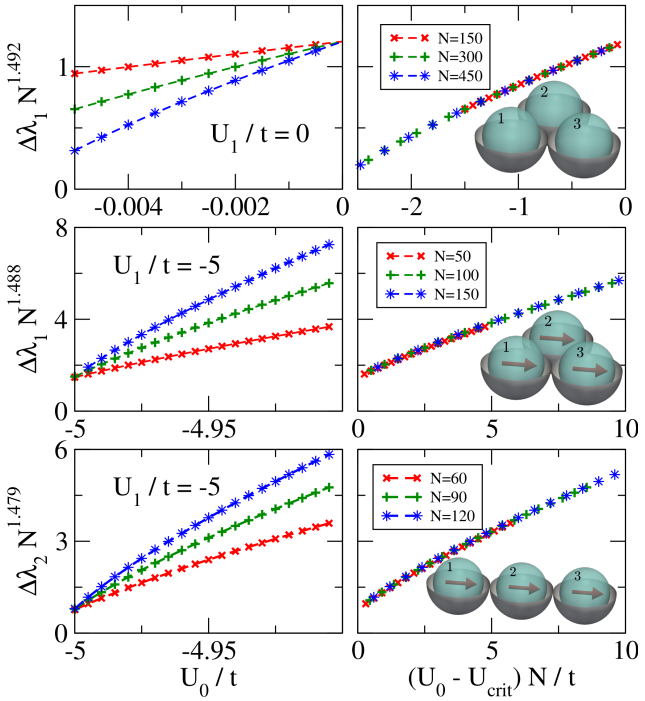

FIG. 4: Finite-size scaling of the Schmidt gap $\Delta\lambda_1$ (top and middle rows) and $\Delta\lambda_2$ (bottom row) for the three configurations displayed in the insets of the right panels. The critical exponents obtained are reported in the text.

systems presented in the previous paragraph, have two independent partitions that lead to two different sets of Schmidt gaps. Following the notation of the labels of the sites in the insets of Fig. 4, $\Delta\lambda_1$ corresponds to the 1/23 partition (1/23 must be read as the partition of site 1 with respect to the subsystem constituted by sites 2 and 3), whereas, $\Delta\lambda_2$ corresponds to the 2/13 partition.

The top (middle) panels of Fig. 4 represent the scaling of $\Delta\lambda_1$ in the triangular non-dipolar (dipolar) case for $N = 150, 300, 450$ ($N = 50, 100, 150$), in the transitions commented above at $U_1 = 0$ ($U_1/t = -5$), where U_1 accounts for the dipole-dipole interaction strength, see Ref. [29] for details. The bottom panels show the scaling of $\Delta\lambda_2$ for the aligned case for $N = 60, 90, 120$. In all three cases, the critical exponents are: $\beta = 3/2$ and $\nu = 1$, which are the same that the ones obtained in the scaling for the double well. As a consequence, they share the universality class with the double-well transition [29]. This property becomes evident for the triangular case with dipolar atoms, where across the QPT analyzed previously, the system behaves as an effective double-well system, with one of the wells completely empty.

V. SUMMARY AND CONCLUSIONS

We have analyzed in this paper the QPTs appearing for mesoscopic BECs trapped in double and in a triple-well configurations. For the former case, the system can

be mapped to the infinite-range Ising model (Lipkin-Meshkov-Glick), and we can define the concept of length and translational invariance in the Hilbert space. This allows us to demonstrate that mean-field QPTs can be also associated to the divergence of a correlation length. Finally, we have generalized our study to the triple-well extended Bose-Hubbard Hamiltonian, which includes also dipolar interactions. We have shown that there exists few QPTs that belong to the same universality class of the double-well (Lipkin-Meshkov-Glick) transition, as reflected by the fact that all the QPTs share the same critical exponents obtained by the scaling properties of the corresponding Schmidt gap. These facts strongly support the suitability of mesoscopic Bose-Einstein condensates as quantum simulators of condensed matter physics.

Acknowledgments

We acknowledge financial support from the Spanish MINECO (FIS2014-52285-C2-1-P and FIS2014-4062-P) and the European Regional development Fund, Generalitat de Catalunya Grant No. SGR2014-401 and SGR2014-946. A. G. is supported by Generalitat de Catalunya Grant FI-DGR 2014 and Spanish MECD fellowship FPU13/02106. We thank useful discussions with G. De Chiara, S. Campbell and M. Moreno-Cardoner.

[1] D. Jaksch, C. Bruder, J. I. Cirac, C. W. Gardiner, and P. Zoller, Phys. Rev Lett. **81**, 3108 (1998).
[2] M. P. A. Fisher, P. B. Weichman, G. Grinstein, and D. S. Fisher, Phys. Rev. B **40**, 546 (1989).
[3] M. Greiner, O. Mandel, T. Esslinger, T. W. Hänsch, and I. Bloch, Nature **415**, 39 (2002).
[4] I. Bloch, J. Dalibard, and W. Zwerger, Rev. Mod. Phys. **80**, 885 (2008).
[5] M. Lewenstein, A. Sanpera, V. Ahufinger, B. Damski, A. D. Sen, and U. Sen, Adv. Phys. **56**, 243 (2007).
[6] M. Lewenstein, A. Sanpera, and V. Ahufinger, *Ultracold Atoms in Optical Lattices. Simulating Quantum Many-Body Systems* (Oxford University Press, 2012).
[7] D. Greif, T. Uehlinger, G. Jotzu, L. Tarruell, and T. Esslinger, Science **340**, 1307 (2013).
[8] J. Simon, W. S. Bakr, R. Ma, M. E. Tai, P. M. Preiss, and M. Greiner, Nature **472**, 307 (2011).
[9] R. Staudt, M. Dzierzawa, and A. Muramatsu, The European Physical Journal B - Condensed Matter and Complex Systems **17**, 411 (2000).
[10] O. Morsch, J. H. Müller, M. Cristiani, D. Ciampini, and E. Arimondo, Phys. Rev. Lett. **87**, 140402 (2001).
[11] M. Albiez, R. Gati, J. Fölling, S. Hunsmann, M. Cristiani, and M. K. Oberthaler, Phys. Rev. Lett. **95**, 010402 (2005).
[12] S. Levy, E. Lahoud, I. Shomroni, and J. Steinhauer, Nature **449**, 579 (2007).
[13] O. Morsch and M. K. Oberthaler, Rev. Mod. Phys. **78**, 179 (2006).
[14] B. Juliá-Díaz, D. Dagnino, M. Lewenstein, J. Martorell, and A. Polls, Phys. Rev. A **81**, 023615 (2010).
[15] P. Ziń, J. Chwedeńczuk, B. Oleś, K. Sacha, and M. Trippenbach, Europhys. Lett. **83**, 64007 (2008).
[16] M. Abad, M. Guilleumas, R. Mayol, M. Pi, and D. M. Jezek, Europhys. Lett. **94**, 10004 (2011).
[17] H. J. Lipkin, N. Meshkov, and A. J. Glick, Nucl. Phys. **62**, 188 (1965).
[18] R. Botet and R. Jullien, Phys. Rev. B **28**, 3955 (1983).
[19] J. Reslen, L. Quiroga, and N. F. Johnson, Europhys. Lett. **69**, 0295 (2005).
[20] S. Dusuel and J. Vidal, Phys. Rev. Lett. **93**, 237204 (2004).
[21] R. Orús, S. Dusuel, and J. Vidal, Phys. Rev. Lett. **101**, 025701 (2008).
[22] S. Sachdev, *Quantum Phase Transitions* (Cambridge University Press, 1999).
[23] G. D. Chiara, L. Lepori, M. Lewenstein, and A. Sanpera, Phys. Rev. Lett. **109**, 237208 (2012).
[24] L. Lepori, G. D. Chiara, and A. Sanpera, Phys. Rev. B **87**, 235107 (2013).
[25] M. E. Fisher and M. N. Barber, Phys. Rev. Lett. **28**, 1516 (1972).
[26] P. Buonsante, R. Burioni, E. Vescovi, and A. Vezzani, Phys. Rev. A **85**, 043625 (2012).
[27] L. Dell'Anna, G. Mazzarella, V. Penna, and L. Salasnich, Phys. Rev. A **87**, 053620 (2013).
[28] A. Gallemí, M. Guilleumas, J. Martorell, R. Mayol, A. Polls, and B. Juliá-Díaz, New J. Phys. **17**, 073014 (2015).
[29] A. Gallemí, M. Guilleumas, R. Mayol, and A. Sanpera, Phys. Rev. A **88**, 063645 (2013).
[30] T. Lahaye, T. Pfau, and L. Santos, Phys. Rev. Lett. **104**, 170404 (2010).